Available online at www.sciencedirect.com
SCIENCE DIRECT
International Journal of Heat and Mass Transfer 49 (2006) 3487–3499
International Journal of HEAT and MASS TRANSFER
www.elsevier.com/locate/ijhmt

Heat transfer during pool boiling based on evaporation from micro and macrolayer

A.K. Das, P.K. Das *, P. Saha

Department of Mechanical Engineering, Indian Institute of Technology, Kharagpur 721302, India

Received 11 October 2005; received in revised form 24 February 2006
Available online 11 May 2006

Abstract

An analytical model of heat transfer based on evaporation from the micro and macrolayers to the vapor bubble during pool boiling is developed. Evaporation of microlayer and macrolayer during the growth of individual bubbles is taken care of by using temporal and spatial variation of temperature in the liquid layer. Change of bubble shape during the entire cycle of bubble growth and departure is meticulously considered to find out the rate of heat transfer from the solid surface to the boiling liquid. Continuous boiling curve is developed by considering the bubble dynamics and decreasing thickness of liquid layer along with the increase of dry spot radius. Transient variation of macrolayer and microlayer thickness is predicted along with their effect on CHF. Present model exhibits a good agreement with reported experimental data as well as theories.

Keywords: Microlayer; Macrolayer; Dry out radius; Critical heat flux; Bubble; Pool boiling

1. Introduction

Boiling heat transfer finds extensive applications in a variety of industries. Metallurgical processing, thermal and nuclear power generation refrigeration, cryogenics and space applications, electronic component cooling are a few to name. Yet boiling heat transfer is one of the least understood topics in thermal engineering. Though a large number of experimental investigations have been made over the years the processes like nucleation, boiling crisis, transition etc. cannot be well explained from the first principle. As a result no well-established theory exists for predicting the rate of heat transfer during boiling. Nevertheless, because of the practical importance of boiling heat transfer, thermal engineers have proposed various phenomenological models based on the insight gained from the experimental observations. In general, these models contain one or more empirical constants and have different level of accuracies for different data sets. Till the complex physics of boiling is understood, there remains a scope for improving such mechanistic models.

Nukiyama [1] first developed the basic understanding of the physical processes that occurs during boiling by heating a nichrome wire in a saturated pool of water. He distinguished different modes of pool boiling such as partial nucleate boiling, fully developed nucleate boiling, transition boiling and film boiling. Out of these fully developed nucleate boiling exhibits a very high rate of heat transfer and the absence of local hot/dry spots—which is very suitable for a large number of industrial processes. Though in most of the heat exchange processes convective boiling is encountered enough efforts have been spared to study pool boiling to develop an understanding of the boiling process as such. Rohsenow [2] was the first to propose a physical model of nucleate boiling as well as a theoretical expression of heat transfer coefficient containing two empirical constant (C_{sf}, s).

$$\frac{c_{pl}\Delta T_{sat}}{h_{fg}Pr^{s}} = c_{sf}\left[\frac{q_w}{\mu h_{fg}}\sqrt{\frac{\sigma}{g(\rho_l-\rho_v)}}\right]^{0.33} \quad (1)$$

* Corresponding author. Tel.: +91 3222 282916; fax: +91 3222 282278.
E-mail address: pkd@mech.iitkgp.ernet.in (P.K. Das).

0017-9310/$ - see front matter © 2006 Elsevier Ltd. All rights reserved.
doi:10.1016/j.ijheatmasstransfer.2006.02.050

Nomenclature

A_d	maximum cross sectional area at the time of departure (m^2)
A_{mi}	microlayer area (m^2)
c_1	change of degree of superheat (K/s)
c	constant stated in Eq. (4) (dimensionless)
C_{pl}	heat capacity (KJ $(kg\ K)^{-1}$)
C_s	empirical constant for bubble departure diameter (dimensionless)
C_{sf}	empirical constant used in Eq. (1) (dimensionless)
d	diameter of the bubble at the end of initial phase (m)
D_d	bubble departure diameter (m)
F_{sy}	surface tension force (N)
F_{duy}	unsteady growth force (N)
F_b	buoyancy force (N)
F_l	lift force (N)
g	acceleration due to gravity ($m\ s^{-2}$)
h_{fg}	latent heat ($J\ kg^{-1}$)
k_l	thermal conductivity $(W\ (m\ K)^{-1})$
K	empirical constant used in Eq. (25) (dimensionless)
n	empirical constant used in Eq. (25) (dimensionless)
Pr	liquid Prandtl number (dimensionless)
$q(r,t)$	wall heat flux as a function of r and t ($W\ m^{-2}$)
q_w	wall heat flux ($W\ m^{-2}$)
q_c	heat flux due to thermal boundary layer ($W\ m^{-2}$)
q_{CHF}	critical heat flux ($W\ m^{-2}$)
r	radial coordinate (m)
r_d	dry out radius (m)
r_c	radius at which superheated boundary layer touches the bubble (m)
R	instantaneous radius of the bubble (m)
R_d	bubble departure radius (m)
s	empirical constant used in Eq. (1) (dimensionless)
t	time (s)
t_d	bubble departure time (s)
t_g	initial growth period (s)
t^*_{mg}	time at which boundary layer touches the liquid vapor interface (s)
T_0	incipient boiling wall temperature (K)
T_w	instantaneous wall temperature (K)
u_b	velocity of the bubble front ($m\ s^{-1}$)
V_b	instantaneous bubble volume (m^3)

Greek symbols

ΔT_{sat}	degree of superheat (K)
α	liquid thermal diffusivity ($m^2\ s^{-1}$)
δ_{mi}	microlayer thickness (m)
δ_{ma}	macrolayer thickness (m)
δ_c	thickness of superheated boundary layer (m)
μ	liquid dynamic viscosity ($kg\ m^{-1}\ s^{-1}$)
ρ_l	liquid density ($kg\ m^{-3}$)
ρ_v	vapor density ($kg\ m^{-3}$)
σ	surface tension of liquid solid combination ($N\ m^{-1}$)
Φ	contact angle

Subscripts

0	initial
1	liquid
v	vapor
d	at a radial position $d/2$

In 1958 Zuber [3] developed a theoretical approach to describe the methodology for determining critical heat flux based on hydrodynamic instability that is known as far field model.

As the process of nucleation depends essentially on the surface condition and the wetting property of the boiling fluid, Mikic and Rohsenow [4] suggested a heat transfer model for flat surfaces which considers micro-conduction only at the nucleation site and natural convection elsewhere.

Katto et al. [5] realized the importance of evaporative heat transfer from thin liquid layers adjacent to the bubbles. They were first to propose a heat transfer model based on macrolayer evaporation. Haramura and Katto [6] and Pan et al. [7] developed their macrolayer model further stating that instability at the macrolayer interface termed, as near field phenomena is the main controlling parameter throughout the boiling process. Among the other efforts of near field model Pasamehmetoglu et al. [8] described the phenomena by the dry out of microlayer (liquid layer of very small thickness below the growing bubble) and macrolayer. Brief reviews stating all these models have been presented by Katto [9] and Lienhard [10].

Lay and Dhir [11] used a vapor stem model which is also based on the evaporation of the microlayer. Currently, Zhao et al. [12] predicted critical heat flux based on a dynamic microlayer model for steady and transient boiling heat transfer. They calculated the microlayer thickness varying with time and space ignoring the heat transfer from macrolayer.

Shoji et al. [13] numerically derived the transient macrolayer thickness and finally predicted the total boiling curve. They considered three-dimensional transient heat conduction to investigate the spatial variation of wall temperature.

Luttich et al. [14] developed a unifying correlation for entire boiling curve using two-phase flow averaging theory. They suggested that volumetric presence of interface close to the heating surface play an important role for overall heat transfer phenomena during boiling. Recently Sateesh et al. [15] developed a model for prediction of heat transfer phenomena over inclined surface as well as horizontal cylinder considering latent heat transfer due to microlayer evaporation, transient conduction due to thermal boundary layer formation, natural convection and heat transfer due to the sliding bubbles. They also suggested that sliding bubbles take an important role during heat transfer over inclined surface or cylindrical surface. Taking the queue from [15], Das and Roetzel [16] developed a composite heat transfer model for pool boiling on horizontal tubes. Their model shows good agreement with experimental result generated by them and reported in literature.

In the present work the near field heat transfer based on the dynamics of micro and macrolayers and the far field heat transfer based on bulk convection as well as transient triple point growth have been combined judicially to build a mechanistic model of pool boiling over horizontal flat surface. Transient temperature variation of the liquid layer below the growing bubble based on Zhao et al. [12] has also been considered. The model is suitable for both transient and steady state heating. The model prediction has been compared with experimental data sets of a number of different sources and encouraging agreements have been observed.

2. Bubble growth model

To develop a generalized saturated pool boiling model formation, growth and departure of a separate bubble have to be considered in details. The assumptions made in carrying out the analysis are as follows:

(I) The heater surface temperature is uniform. Transient variation of temperature is directly proportional with time.
(II) Horizontal and vertical interactions between the bubbles are not considered. It is assumed that the generation of single bubbles from each nucleation site is not influenced by the surrounding conditions.
(III) Liquid replenishment is continuous and motion of liquid beneath the bubble during this phase does not affect the bubble formation and its growth.
(IV) Liquid to be evaporated is homogeneous and its property is not changing with time and temperature.
(V) Ideal gas law is applicable for the vapor phase.

Based on the observations reported by Cooper and Lloyd [17] a phenomenological model of bubble growth and departure has been considered. Just after nucleation one can assume the vapor bubble as a small hemisphere just above the nucleation site. At this moment it is fed solely from the nucleation site. As the vapor bubble increases in size it presumable retains its hemispherical shape but a wedge shaped liquid layer known as microlayer forms below the base of the vapor bubble. Evaporation from this thin microlayer increases the bubble size and extends its radius. This also increases the radial expense of the microlayer. Microlayer adjacent to the nucleation site starts evaporating completely increasing the dry out area at the base of the bubble. At this stage the vapor bubble retains its approximate hemispherical shape due to its equal movement of the vapor phase along the radial direction (Fig. 1).

When the heating surface gains a certain degree of superheat the enhanced rate of evaporation forces the centre of the bubble to shift upward. This reduces the growth of the microlayer a great extent and initiates the second phase of bubble growth where heat transfer from the macrolayer plays a dominant role. Conventionally the liquid layer starting from the edge of the microlayer to the outer edge of the vapor bubble (shown in Fig. 2.) is termed as macrolayer. In this period movement of the vapor particle in the direction parallel to the surface is going to decrease in comparison to its movement in the perpendicular direction, this transforms the hemisphere to truncated sphere. Final growth stage is governed mainly by the

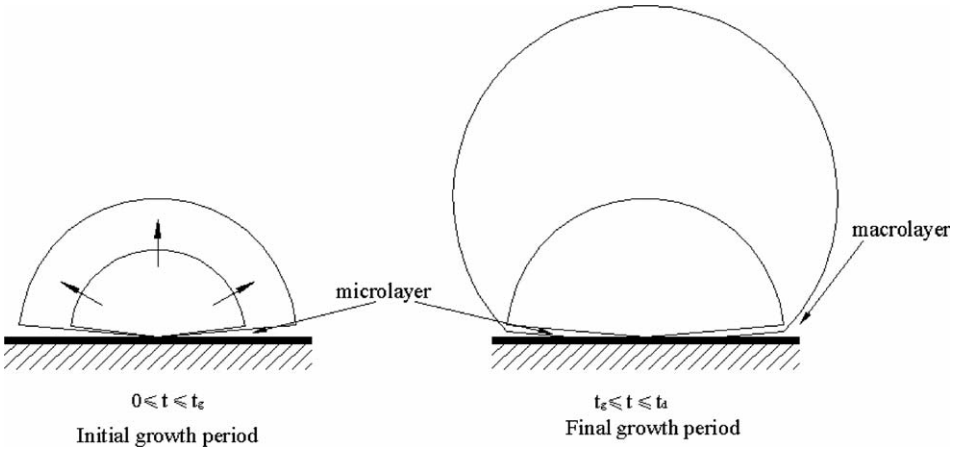

Fig. 1. Various phase of bubble cycle.

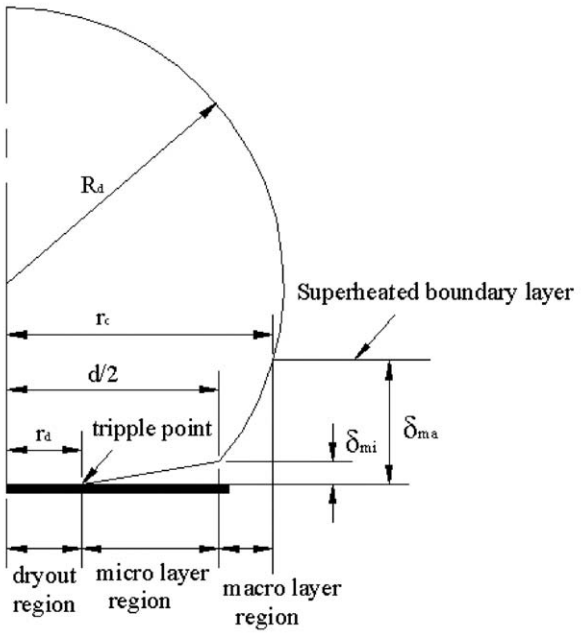

Fig. 2. Different regions of heat transfer for a single bubble growth.

hydrodynamics. Radial location of macrolayer front increases continuously till the superheated boundary layer touches the liquid vapor interface. Beyond this period external heat flux takes the main role for the increment of bubble diameter.

At the final growth stage microlayer thickness near the line of symmetry diminishes that creates a triple point circle. Inside this triple point circle heat is transferred to the vapor from the heating surface. It is quite negligible in comparison to the other modes of heat transfer.

From Fig. 2 it can be said that basically the heating surface beneath the individual bubble is divided into three separate segments namely dry out region, microlayer region and macrolayer region. For low degree of super heat microlayer evaporation is the main mode of heat transfer. But with the increase of temperature macrolayer evaporation as well as external heat flux also becomes significant in the heat transfer process. The individual area of above said regions changes with time. Dry out radius starts from zero and increases causing the internal radius of the microlayer to increase. Outer radius of the microlayer increases during the initial growth period after that it stops. Macrolayer thickness is zero throughout the initial growth period. At the final growth period it starts to build and continues till the departure of the bubble. During the departure of the bubble two types of coalescence occurs. At the low superheat region horizontal coalescence happens, as the frequency of the bubble is low. With the increase of degree of superheat vertical coalescence with the previous bubble from the same site occurs. However, these coalescences do not alter the evaporation mechanism from the heating plate though they influence the local flow field drastically.

Local surface heat flux for a given degree of superheat has to be calculated first. It can be written as

$$q(r,t)=\begin{cases}0 & r\leqslant r_d\\ -\rho_l h_{fg}\frac{d\delta_{mi}}{dt} & r_d\leqslant r\leqslant d/2\\ -\rho_l h_{fg}\frac{d\delta_{ma}}{dt} & d/2\leqslant r\leqslant r_c\\ q_c & D_d\geqslant r\geqslant r_c\end{cases} \tag{2}$$

Here q_c is the rate of external heat transfer and it comes into existence from the radius r_c, which is the radius where super heated liquid layer touches the bubble. It can be calculated considering periodical transient heat conduction in a semi-infinite liquid layer. The dry out radius or the location of the triple point r_d advances outward as the degree of superheat increases.

A generalized variation of surface temperature in the following form is considered:

$$T_w=T_{sat}+T_0+c_1 t \tag{3}$$

Here T_0 is the boiling incipient temperature and c_1 is a constant, which denotes the change of temperature of the heating surface with respect to time.

The mean wall heat flux can be derived accordingly using Eq. (4).

$$\begin{aligned}\bar{q}_w=\frac{1}{A_d t_d}\Bigg[&\int_0^{t_d}\int_{A_{mi}}\left(-\rho_l h_{fg}\frac{d\delta_{mi}}{dt}\right)dA\,dt\\&+\int_0^{t_d}\int_{\pi r_c^2-A_{mi}}\left(-\rho_l h_{fg}\frac{d\delta_{ma}}{dt}\right)dA\,dt\\&+\int_0^{t_d}\int_{\frac{\pi}{4}\left(D_d^2-r_c^2\right)} q_c\,dA\,dt\Bigg]\end{aligned} \tag{4}$$

It may be noted that the mean wall heat flux is a complex function of a number of physical parameters that are in turn functions of process parameters and fluid properties. In a generalized functional form Eq. (4) can be written as

$$\bar{q}_w=f(D_d,t_d,\delta_{mi}(r,t),\delta_{ma}(r,t),q_c(\Delta T)) \tag{5}$$

The parameters appearing in the left hand side of the equation needs to be evaluated separately. The procedure is elaborated below.

2.1. Evaporation of microlayer

Cooper and Lloyd [17] derived the expression for initial microlayer thickness neglecting the surface tension effect:

$$\delta_{mi}^0=0.8\sqrt{v_l t}=\sqrt{c\alpha t},\quad 0\leqslant t\leqslant t_g \tag{6}$$

where $c=0.64Pr$.

Equating the evaporation of microlayer and the heat conduction [12] through it, governing equation for the initial growth period can be developed.

$$\frac{2}{3}\pi R^3\rho_v h_{fg}=2\pi k_l\int_0^R\int_{\tau_g}^t\frac{\Delta T_{sat}}{\delta_{mi}}r\,dt\,dr,\quad 0\leqslant t\leqslant t_g \tag{7}$$

Time τ_g is required for the hemispherical bubble of radius R to reach the radial position r ($r=R$). For the nucleate boiling region this time is very small so that we can neglect it. Then the following approximation can be made:

$$\frac{2}{3}\pi R^3\rho_v h_{fg} = 2\pi k_l \int_0^R \int_0^t \frac{\Delta T_{sat}}{\delta_{mi}} r\,dt\,dr, \quad 0 \leqslant t \leqslant t_g \tag{8}$$

From Cooper's equation of initial microlayer thickness the bubble radius for the initial growth period may be evaluated.

$$R \equiv r = \frac{2k_l\left(T_0 + \frac{c_1 t}{7}\right)}{\rho_v h_{fg}\sqrt{c\alpha}} t^{1/2}, \quad 0 \leqslant t \leqslant t_g \tag{9}$$

The above equation gives,

$$t = f(r) = \left[\frac{r\rho_v h_{fg}\sqrt{c\alpha}}{4k_l} + \left(\frac{T_0^3}{27} + \left(\frac{r\rho_v h_{fg}\sqrt{c\alpha}}{4k_l}\right)^2\right)^{\frac{1}{2}}\right]^{\frac{2}{3}} + \left[\frac{r\rho_v h_{fg}\sqrt{c\alpha}}{4k_l} - \left(\frac{T_0^3}{27} + \left(\frac{r\rho_v h_{fg}\sqrt{c\alpha}}{4k_l}\right)^2\right)^{\frac{1}{2}}\right]^{\frac{2}{3}} + \frac{2T_0}{3} \tag{10}$$

At the end of initial growth period, i.e. when the bubble front reaches the diameter d the final growth period starts. Bubble diameter at the end of initial phase (d) can be evaluated as

$$d = \frac{4k_l\left(T_0 + \frac{c_1 t_g}{7}\right)}{\rho_v h_{fg}\sqrt{c\alpha}} t_g^{1/2} \tag{11}$$

Eqs. (3) and (10) can be used to evaluate the initial microlayer thickness as a function of radial coordinate:

$$\delta_{mi}^0 = \sqrt{c\alpha f(r)} \tag{12}$$

Now after the formation of microlayer it gradually evaporates into the bubble above due to the conduction from the heating surface.

It can be stated as

$$-\rho_l h_{fg}\frac{d\delta_{mi}}{dt} = \frac{k_l \Delta T_{sat}}{\delta_{mi}} \tag{13}$$

With the boundary condition at $t = t_g$, $\delta_{mi} = \delta_{mi}^0$.

Then the thickness of the microlayer can be evaluated as a function of time and the radial position [12]:

$$\frac{\delta_{mi}(r,t)}{\sqrt{c\alpha f(r)}} = \left\{\frac{1 - 2k_l\left[T_0(t - f(r)) + \frac{c_1(t-f(r))^2}{2}\right]}{\rho_l h_{fg}}\right\}^{\frac{1}{2}} \tag{14}$$

2.2. Evaporation of macrolayer

Formation of macrolayer starts at the end of initial growth period. Defining R as the radius of the bubble after initial growth initial thickness of macrolayer can be described as

$$\delta_{ma}^0 = \sqrt{R^2 - \left(\frac{d}{2}\right)^2} + \delta_{mi}^d - \sqrt{R^2 - r^2} \tag{15}$$

In the final growth period macrolayer also takes part in evaporation and feeds the growing bubble. Accordingly one gets

$$-\rho_l h_{fg}\frac{d\delta_{ma}}{dt} = \frac{k_l \Delta T_{sat}}{\delta_{ma}} \tag{16}$$

with the initial condition: $\delta_{ma} = \delta_{mi}$ at $t = t_{mg}^*$.

Here t_{mg}^* is the time at which superheated boundary layer reaches the liquid vapor interface that can be calculated using thickness of the boundary layer for a fixed degree of superheat.

$$\pi\alpha t_{mg}^* = \frac{2k_l}{\rho_l h_{fg}}\left[T_0(t - t_{mg}^*) + \frac{c_1(t - t_{mg}^*)^2}{2}\right] \tag{17}$$

From the above quadratic equation t_{mg}^* can be obtained as follows:

$$t_{mg}^* = \frac{-b + \sqrt{b^2 - 4ac}}{2a} \tag{18}$$

where $a = \frac{k_l c_1}{\rho_l h_{fg}}$, $b = \left[-\pi\alpha - \frac{2k_l T_0}{\rho_l h_{fg}} - \frac{2k_l c_1 t}{\rho_l h_{fg}}\right]$ and $c = \frac{2k_l T_0 t}{\rho_l h_{fg}}$. Now from Eqs. (15)–(18) it can be written that

$$\delta_{ma}(r,t) = \left\{\left(\sqrt{R^2 - \left(\frac{d}{2}\right)^2} + \delta_{mi}^d - \sqrt{R^2 - r^2}\right)^2 - \frac{2k_l}{\rho_l h_{fg}}\left[T_0(t - t_{mg}^*) + \frac{c_1(t - t_{mg}^*)^2}{2}\right] + \left(d + \sqrt{c_1\alpha t_{mg}^*}\right)\left(d + \sqrt{c_1\alpha t_{mg}^*} - \frac{2c_1\alpha t_{mg}^*\cot^2\phi}{d}\right)\right\}^{\frac{1}{2}} \tag{19}$$

2.3. Transient heat conduction

When superheated boundary layer reaches the liquid vapor interface heat flux can be calculated by transient heat conduction within the liquid layer. The transient heat conduction can be calculated as

$$q_c = \frac{k_l}{\sqrt{\pi\alpha}}\left[\frac{\Delta T_{sat}(t)}{\sqrt{t}} + \frac{1}{2}\int_0^t \frac{\Delta T_{sat}(t) - \Delta T_{sat}(\xi)}{(t-\xi)^{\frac{3}{2}}} d\xi\right] \tag{20}$$

With the help of Eq. (3) and simplifying Eq. (20) one gets

$$q_{cd} = \frac{k_l}{\sqrt{\pi\alpha}}\left[\frac{T_0}{\sqrt{t}} + 2c_1\sqrt{t}\right] \tag{21}$$

To evaluate the transient heat conduction, the radial position of the intersection point of superheated boundary layer and vapor bubble interface is necessary. From Fig. 2 one may write:

$$r_c = \sqrt{R^2 - \left[\left(R^2 - \frac{d^2}{4}\right)^{\frac{1}{2}} + \delta_{mi} - \delta_c\right]^2} \tag{22}$$

Here δ_c is the thickness of the superheated boundary layer.

For uniform heat flux, $\delta_c = \sqrt{\pi\alpha t}$.

2.4. Bubble departure radius

Dynamics of a growing bubble is complex as a large number of forces of different magnitude acts on it. Consulting the models of Ramaswamy et al. [18] and Van Stralen et al. [19] the momentum equation for a departing bubble can be expressed as

$$F_{sy} + F_{duy} + F_b + F_L = \rho_v V_b \frac{du_{bc}}{dt} \tag{23}$$

Left hand side of the above equation denotes the bubble inertia force; however the contribution due to changing bubble radius has been neglected.

Van Stralen et al. [19] stated that among all the forces unsteady growth force and buoyancy forces are significant. According to Zeng et al. [20] F_{duy} can be expressed as

$$F_{duy} = -\rho_l \pi r^2 \left(\frac{3}{2} C_s \dot{r}^2 + r\ddot{r}\right) \tag{24}$$

C_s is an empirical constant whose value has been suggested as $\frac{20}{3}$ [20] based on a best fit of the pool boiling data. Buoyancy force F_b is written as

$$F_b = \frac{4}{3}\pi r^3 (\rho_l - \rho_v) g \tag{25}$$

In general vapor bubble growth rate follows a power law

$$r(t) = Kt^n \tag{26}$$

According to Zeng et al. [20] empirical value of K and n are 0.00444 and 0.38 accordingly. Now balancing F_b and F_{duy} one can get

$$D_b = 2\left\{\frac{3}{4}\frac{K_n^2}{g}\left[\frac{3}{2}C_s n^2 + n(n-1)\right]\right\}^{n/(2-n)} \tag{27}$$

3. Result and discussion

Variation of microlayer thickness for three different rates of transient heat input using water as the working fluid is plotted in Fig. 3. Here the microlayer thickness at the location of $d/2$ is nondimensionalized by the initial microlayer thickness at that position. With the passage of time the thickness decreases due to evaporation causing the increase in the bubble diameter. Microlayer evaporation increases with the rate of heat input as expected. The trend of microlayer evaporation is also matches with that predicted by Zhao et al. [12].

Corresponding changes of macrolayer thickness is depicted for a fixed radial location ($3d/2$) in Fig. 4. Macrolayer thickness at any instant is nondimensionalized by the initial macrolayer thickness for the corresponding location. At the end of initial period macrolayer starts to generate and it causes the increase of the bubble diameter. For a particular radial position there will be no evaporation along the axial direction from liquid vapor interface until the interface reaches there. Macrolayer thickness will be defined at any position when existence of macrolayer is traceable at that radial location. With the increase of the bubble size and the thickness of the superheated boundary layer, extreme point of macrolayer will traverse along the radial direction and for any radial direction macrolayer

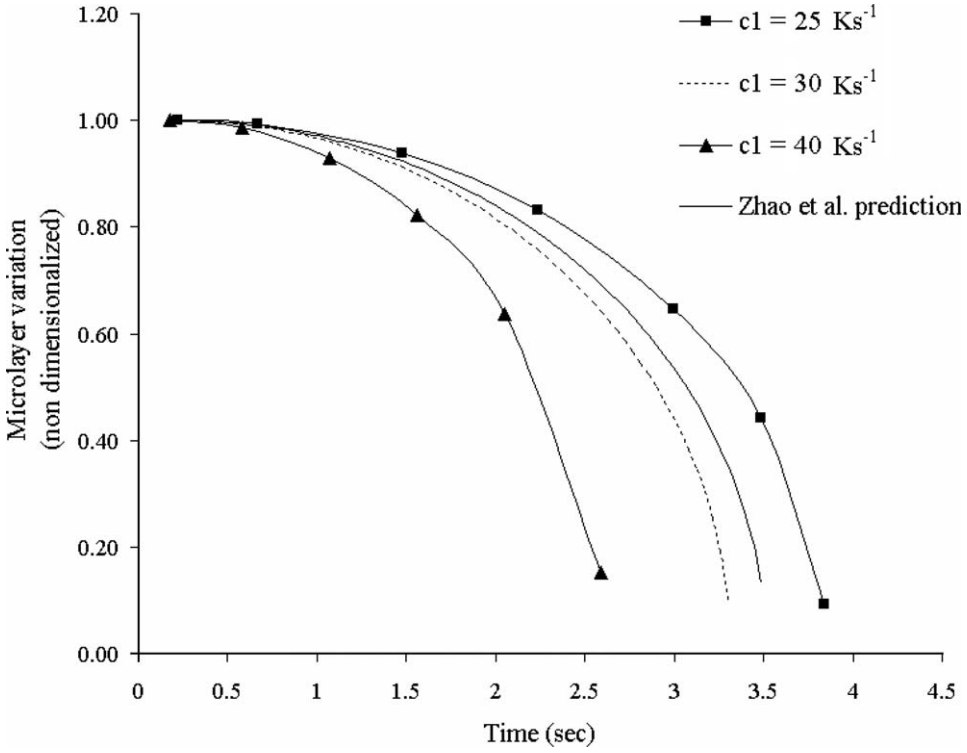

Fig. 3. Prediction of microlayer thickness of water for various heat input rate.

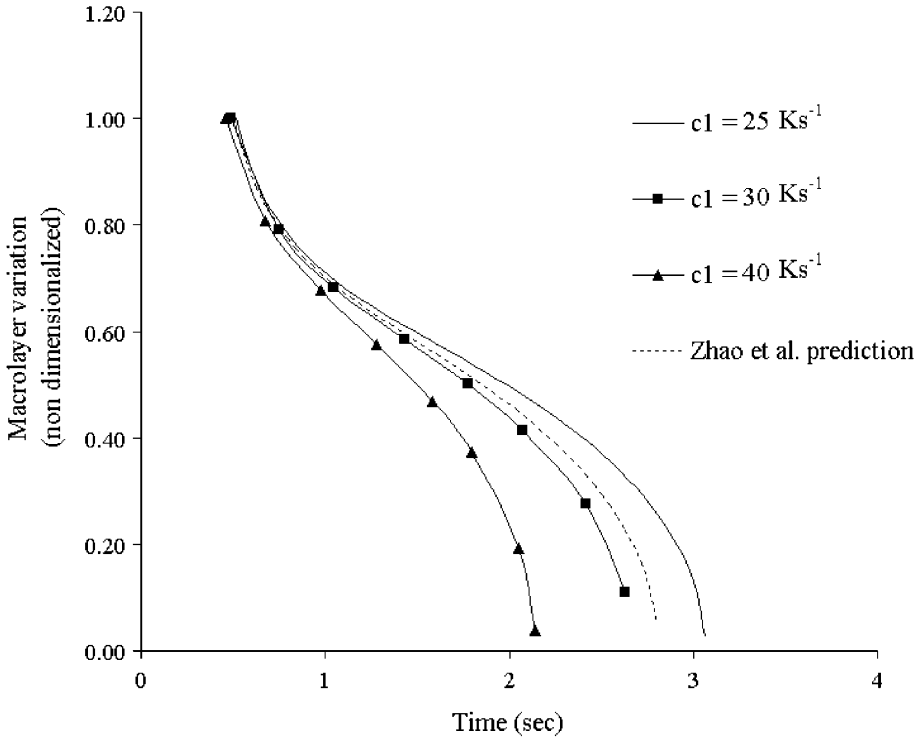

Fig. 4. Prediction of macrolayer thickness of water for various heat input rate.

evaporation will not be considered until macrolayer reaches that position.

When vapor front reaches that position, the thickness of the macrolayer becomes maximum and then it starts decreasing in a similar way to the microlayer. From both microlayer thickness variation (Fig. 3) and macrolayer variation (Fig. 4) it can be seen that prediction of Zhao et al. [12] (for constant wall temperature) lies between 25 K/s and 30 K/s. For large value of c_1 prediction result is deviating due to the rapid heat input. It is also noticeable that with the increase of heat input rate thickness of both the macrolayer and microlayer decreases. It is quite justified due to the fast evaporation of the liquid layer for the higher heat input rate.

Temporal variation of vapor bubble diameter with respect to bubble departure diameter is shown in Fig. 5. The heat input rate on bubble departure has the same effect as it were in case of micro and macrolayer evaporation. It may be noted that the departure diameter of the bubble at a lower heat input rate is larger and it stays on the heating surface for a longer period.

Fig. 6 shows the effect of microlayer on the total wall heat flux. At a lower degree of super heat (less than 9 °C) microlayer evaporation is the only mode of heat transfer because macrolayer does not form at that temperature. For this reason we are only concentrating in a region where both macro and microlayer evaporation takes part (above 9 °C). For a moderate degree of superheat the effect of the macrolayer is going to dominate due to the shift of triple point on the heating surface. With the increase of degree of superheat macrolayer thickness of the extreme end increases reducing the heat transfer from it. Above 20 °C superheat again microlayer dominates over macrolayer evaporation as the change of thickness of microlayer is much greater than macrolayer in that region. Effect of microlayer heat transfer on the process of boiling has also been estimated using the model of Zhao et al. [12] (dotted line in Fig. 6.) and identical trend has been observed.

At a higher degree of superheat microlayer thins down increasing the rate of heat transfer substantially. Eventually entire microlayer evaporates. This maximizes the dry out radius and prompts the occurrence of critical heat flux.

Using Eqs. (14), (19) and (20) wall heat flux can be calculated from Eq. (4). For the calculation, rate of change of temperature (c_1) and the diameter (d) corresponding to the termination of microlayer growth are the inputs. Critical heat flux can be determined from estimating the heat flux with increasing degree of superheat. Success of any mechanistic model depends on its capability of predicting the experimental results. To verify the capability of our model we first consider the experimental data reported by Shoji et al. [13]. Three data sets for water, steady state boiling as well as higher (80 K/s) and lower (5 K/s) heat input rate have been considered. Comparisons are shown in Fig. 7. It may be noticed that though for all the heat input rates the model predicts the correct trend of boiling heat transfer there are considerable quantitative differences for the curves with transient heating. At this point the decision was taken to tune the model instead of modifying the physics underlying it. An exercise was made to examine the

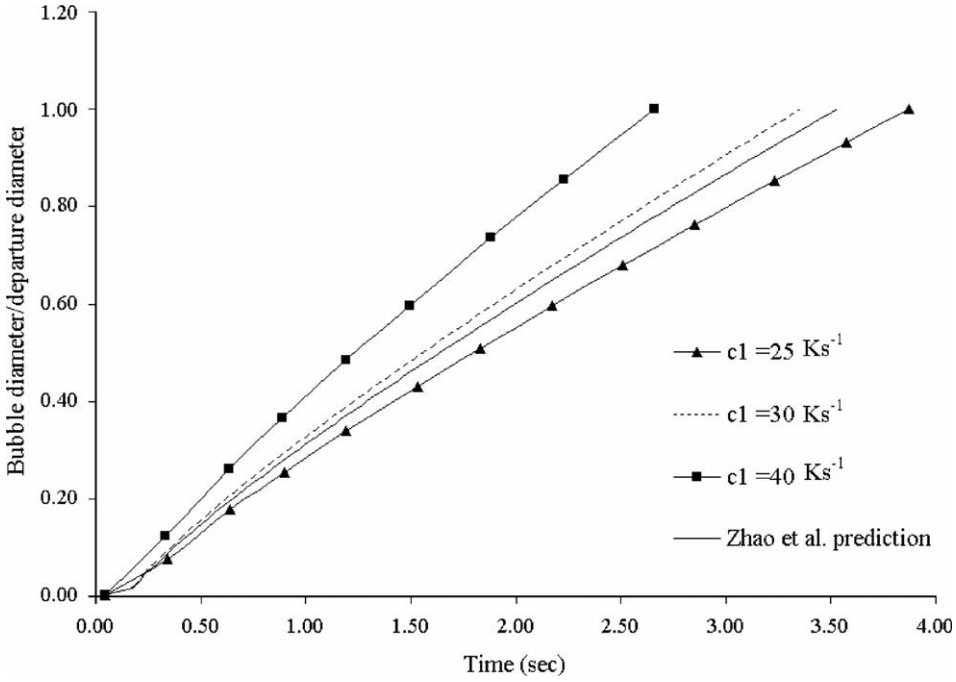

Fig. 5. Variation of instantaneous bubble diameter for water.

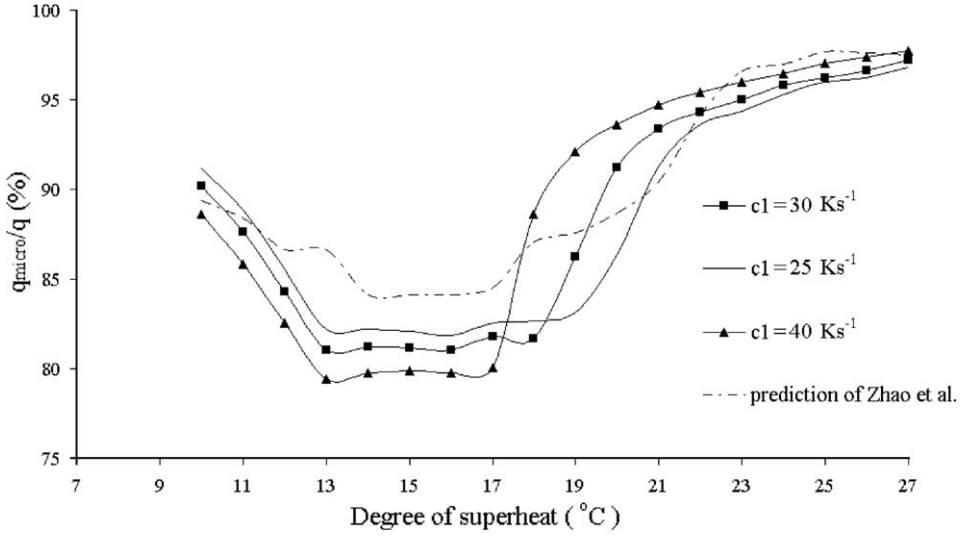

Fig. 6. Effect of microlayer on the wall heat flux for various superheats.

sensitivity of the various empirical co-efficient used in the model. Based on the experimental data for water reported by Shoji et al. [13] it has been observed that the prediction is most sensitive to the constant C_s used in the bubble growth Eq. (24) [20]. Zeng et al. [20] got the value of C_s correlating the pool boiling data for various refrigerants. According to our exercise a value of C_s is equal to 4.0 gives reasonable prediction for water. Improvement in model prediction using the tuned value of C_s can be seen from Figs. 8–10 respectively. In all the three cases the model predicts the nucleate boiling region, critical heat flux and the transition boiling very well. For all the predictions reported in this work the same tuned value of C_s have been used.

In Fig. 11 proposed model for different values of moderate heat input rates are compared with some existing experimental investigations for water. The prediction of the present model agrees well with the experimental results of Sakurai [21] and Gaertner [22]. It needs to be mentioned that tuned value of C_s has been kept unaltered in these cases. A curiosity was also felt to check the model prediction with the well known correlation of nucleate boiling proposed by Rohsenow. Fig. 11 also depicts the Rohsenow correlation with different values of C_{sf} that envelopes our prediction.

Comparison of the critical heat flux for $c_1 = 25$ K/s is shown with the existing correlations of Rohsenow–Griffith,

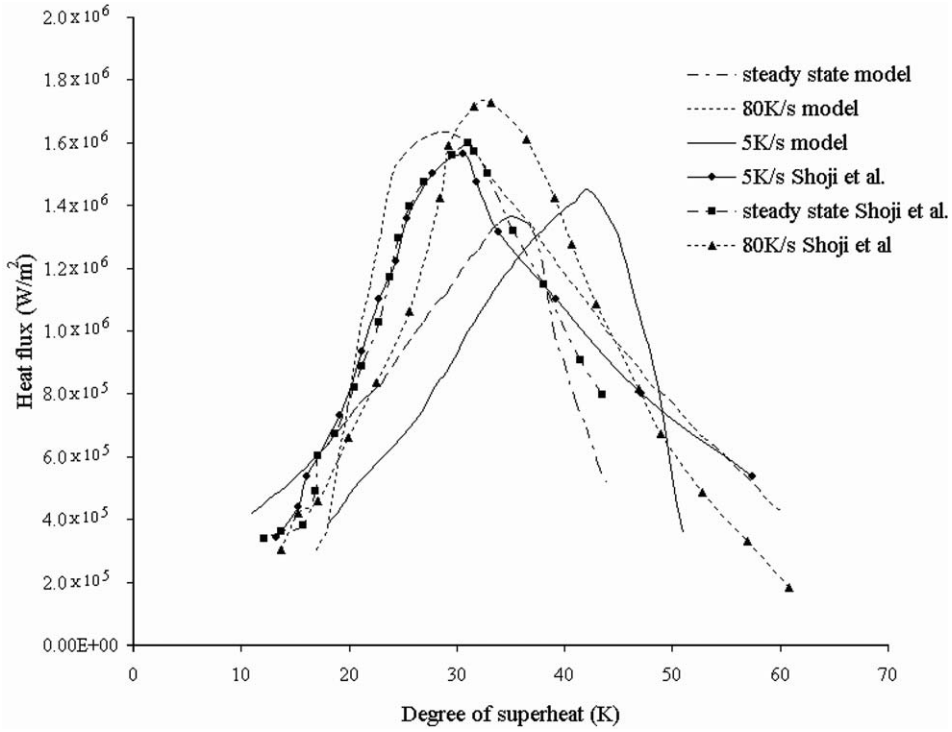

Fig. 7. Comparison of boiling curve for steady state, high and low heat input rate ($C_s = 20/3$).

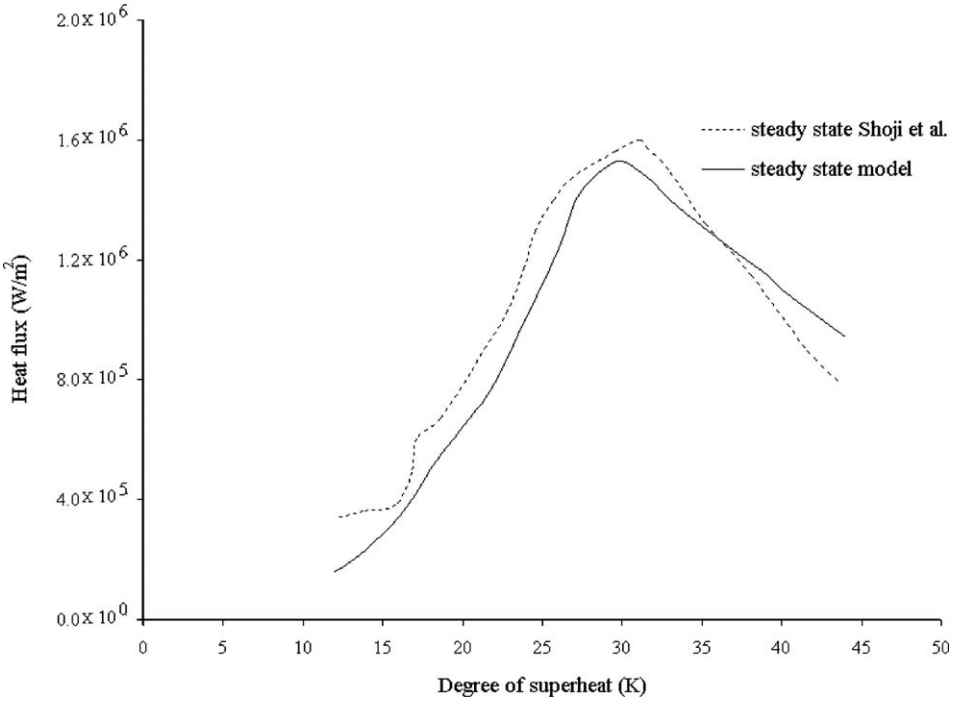

Fig. 8. Comparison of boiling curve for steady state condition ($C_s = 4.0$).

Lienherd, and Kutateladge in Fig. 12. It shows that for a 0.3 mm value of bubble diameter (d), at the end of initial growth phase all the correlations matches well with the prediction. It further shows the critical heat flux is a strong function of bubble diameter (d) and is inversely proportional to it.

The dependence of critical heat flux on bubble diameter (d) has also been established experimentally. Fig. 13 shows

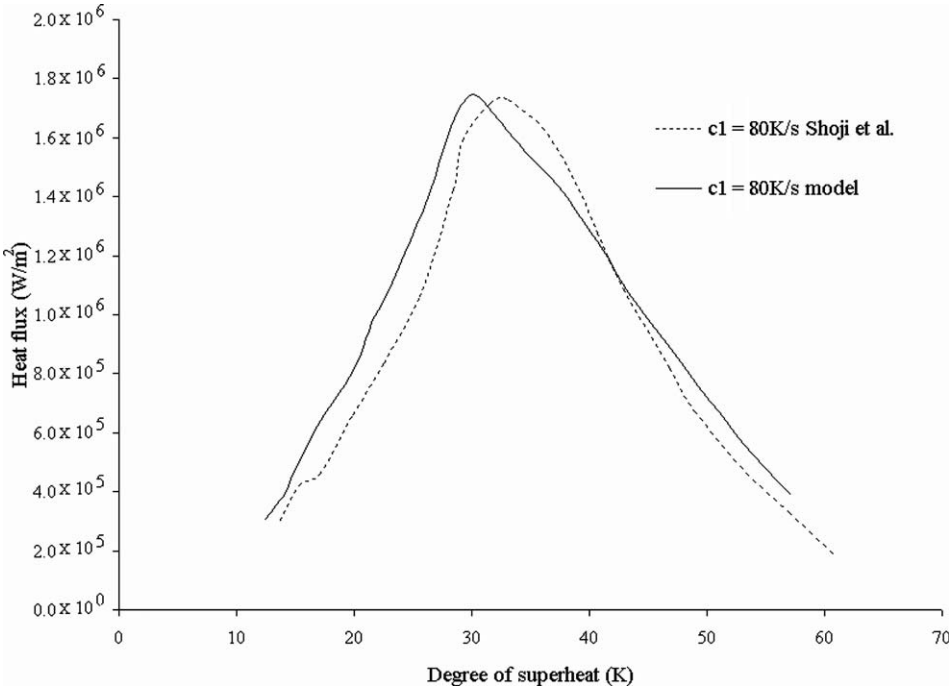

Fig. 9. Comparison of boiling curve for higher heat input rate ($C_s = 4.0$).

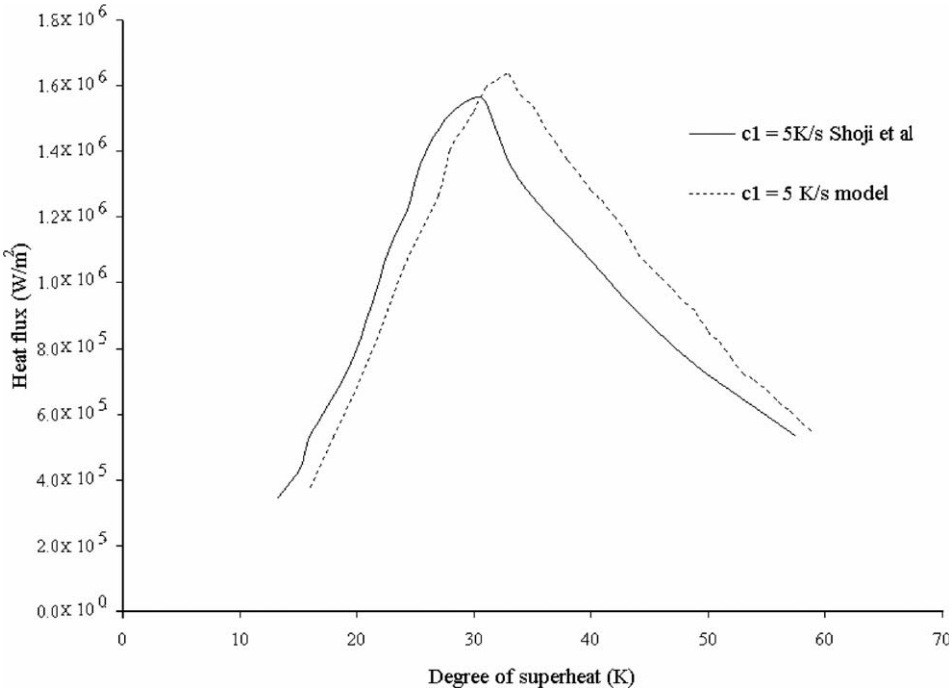

Fig. 10. Comparison of boiling curve for lower heat input rate ($C_s = 4.0$).

the typical dependence of CHF on d as observed by Gaertner [22] for water. The present model agrees well with the data of Gaertner [22] and the prediction is better than that of Zhao et al. [12] model. A regression analysis gives the dependence of CHF on d by the following equation.

$$q_{CHF} = 2876.45 d^{-0.76} \tag{28}$$

Boiling on tubular surface is very important for industrial applications. However, the curvature effect of the tube and the convection pattern around a horizontal tube due to bubble growth and departure may have a significant effect on boiling heat transfer. A model developed for plane surface may therefore be not applicable for horizontal tube. Recently Das and Roetzel [16] developed a composite heat

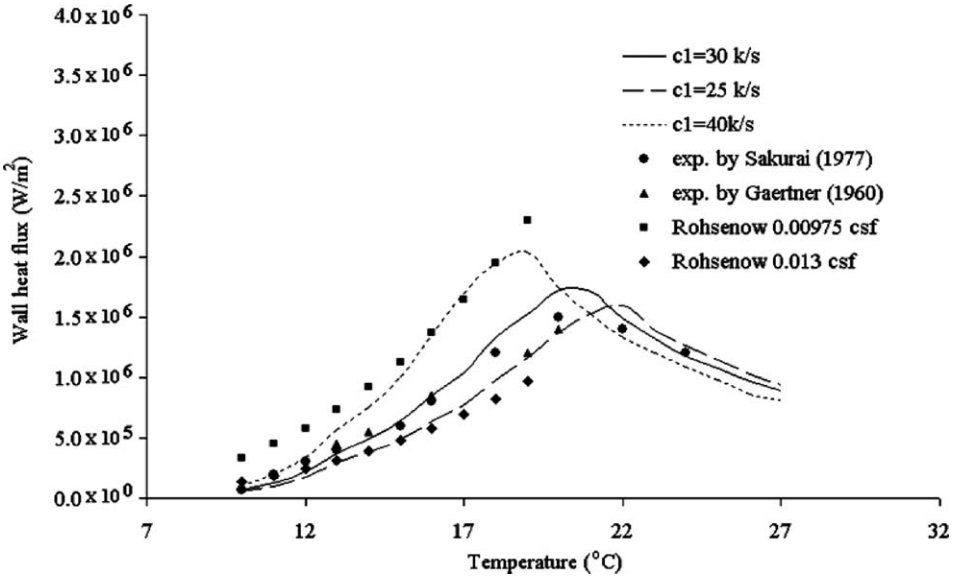

Fig. 11. Comparison of heat flux variation for different rate of change of wall temperature taking water as working fluid.

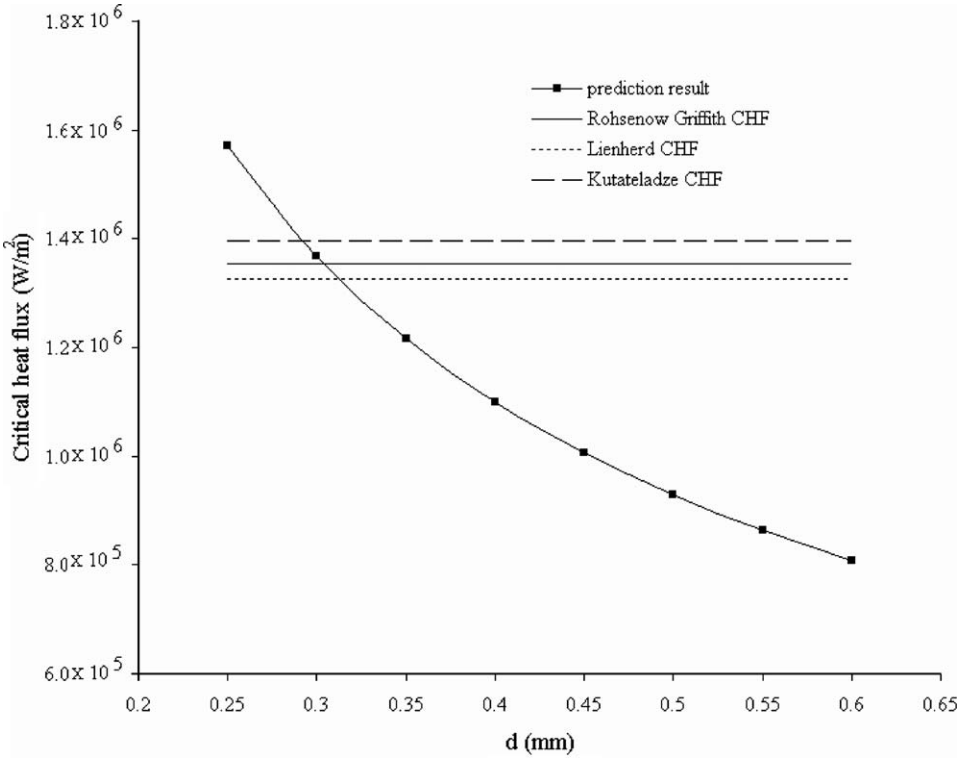

Fig. 12. Comparison with existing correlations of CHF.

transfer model for pool boiling on a horizontal tube for moderate pressure. They have compared the model prediction with experimental data for two tubes of 20 mm and 16 mm respectively. However, the heat transfer values are not much different for different diameters. We wanted to check the applicability of our model for a tubular surface. A comparison of the present model with the experimental data of Das and Roetzel [16] for water boiling over a 20 mm diameter tube shows a good agreement in Fig. 14. If the tube diameter is not too small the curvature effect on the macro and microlayer may be neglected. In this case the tube behaves like a plane surface. But for small diameter tube bubbles emerging through the neighboring sites interact with each other and a departing bubble

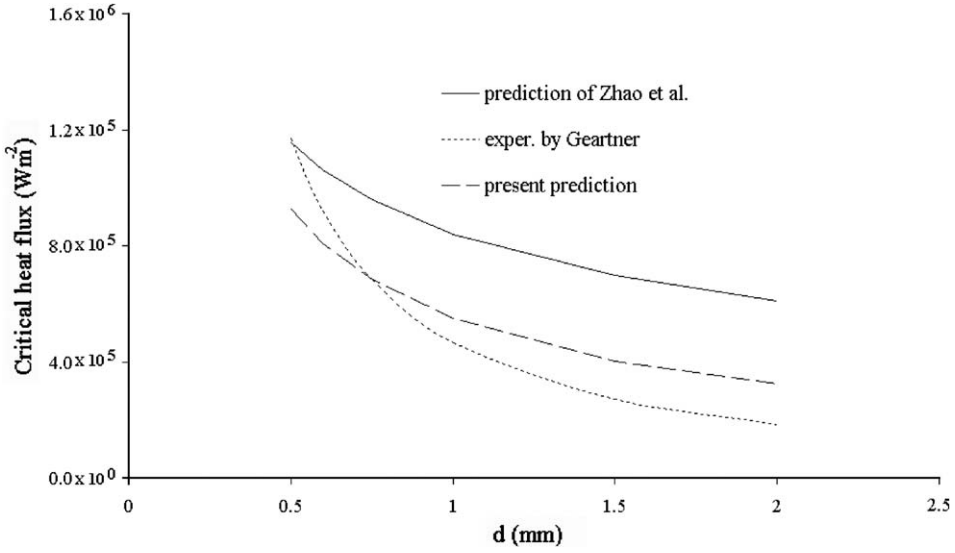

Fig. 13. Prediction of CHF vs. d for water for $c_1 = 25$ K/s.

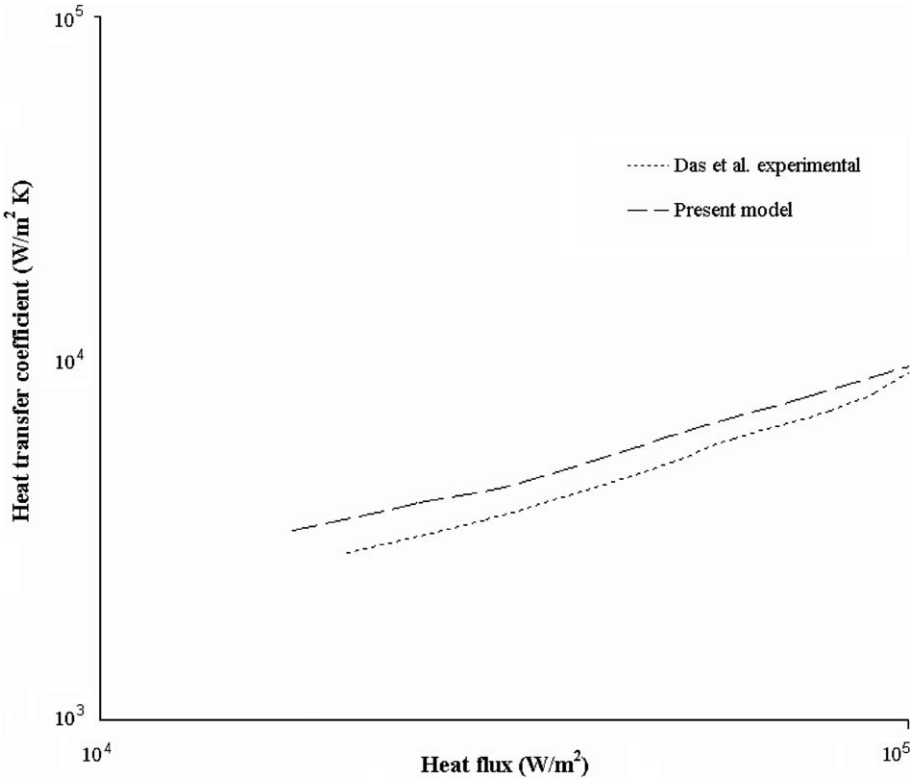

Fig. 14. Comparison of heat flux variation of present model and boiling over a 20 mm diameter tube.

(particularly from the bottom surface of the tube) may substantially change the local flow field. This violates the initial assumptions of the present model.

The experimental data of Das and Roetzel [16] which have been taken for comparison of the present model are for a small range of degree of superheat. An examination of Fig. 14 reveals that the degree of superheat ranges up to only 10 °C. At higher surface temperature poor agreement of the model due to higher bubble density cannot be ruled out. More investigations is necessary in this direction.

4. Conclusion

A mechanistic model has been developed for predicting the heat transfer during pool boiling from a plane

horizontal surface. Dynamic evaporation from the micro and the macrolayer has been considered as the main mechanism of heat transfer from the surface to the growing bubbles. A growing dry out radius defined by a triple point line and its effect have been included in the model. It has been assumed that transient conduction from the surrounding liquid also plays a role in evaporation at the final stage of the bubble growth. The present model is suitable for both steady and transient heating.

The model uses number of empirical constants, which have been taken from earlier literatures. Prediction of model has been examined with the steady state and transient pool boiling data reported by Shoji et al. [13]. To improve the quantitative matching between experiment and theory sensitivity of all the empirical constants used in the model have been examined. Based on this exercise a single empirical constant C_s (Eq. (24)) have been identified and tuned. Using a unique tuned value, the model has been used to simulate heat transfer for pool boiling of water. The simulation correctly depicts the trend for the nucleate boiling, critical heat flux and the transition boiling. The simulation exhibits very good agreement with experimental results taken from different sources.

A correlation has also been developed to predict the CHF based on the bubble diameter at the end of initial growth period. It predicts the experimental data of Gaertner [22] better than earlier model [12]. However, already there exist a number of models for the prediction of critical heat flux. The present technique has to be tested further and improved upon, if necessary, before it is prescribed for the estimation of CHF.

The present model, though developed for plane horizontal surface, has been used to predict the experimental data reported for pool boiling on a horizontal circular cylinder. A good match between the two indicates that the model may be used for cases where the curvature effect is not excessive.

The present mechanistic model of nucleate boiling is based on a few simplified assumptions. It ignores the influence of adjacent bubbles on a particular growing bubble. However, such an assumption is not valid for high heat flux condition where coalescence between the adjacent bubbles is most probable. The model does not take the fluid motion into account and needs a number of empirical constants. Further improvement in the model is required to obviate the above shortcomings.

Acknowledgement

The financial support extended by M.H.R.D., India towards the project is gratefully acknowledged.

References

[1] S. Nukiyama, The maximum and minimum values of the heat transmitted from metal to boiling water under atmospheric pressure, J. Jpn. Soc. Mech. Eng. 37 (1934) 367–374.
[2] W.M. Rohsenow, A method of correlating heat transfer data for surface boiling of liquids, Trans. ASME J. Heat Transfer 74 (1952) 969–976.
[3] N. Zuber, On the stability of boiling heat transfer, Trans. ASME J. Heat Transfer 8 (3) (1958) 711–720.
[4] B.B. Mikic, M. Rohsenow, A new correlation of pool boiling data including the effect of heating surface characteristics, J. Heat Transfer 91 (1969) 245–250.
[5] Y. Katto, S. Yokoya, M. Yasunaka, Mechanism of boiling crisis and transition boiling in pool boiling, in: Proc. 4th Int. Heat Transfer Conf., Paris, France, vol. 5, 1970, p. B3.2.
[6] Y. Haramura, Y. Katto, A new hydrodynamic model of critical heat flux, applicable widely to both pool and forced convection boiling on submerged bodies in saturated liquids, Int. J. Heat Mass Transfer 26 (1983) 389–399.
[7] C. Pan, J.Y. Hwang, T.L. Lin, The mechanism of heat transfer in transition boiling, Int. J. Heat Mass Transfer 32 (1989) 1337–1349.
[8] K.O. Pasamehmetoglu, P.R. Chappidi, C. Unal, R.A. Nelson, Saturated pool nucleate boiling mechanisms at high heat fluxes, Int. J. Heat Mass Transfer 36 (1993) 3859–3868.
[9] Y. Katto, Critical heat flux, Int. J. Multiphase Flow 20 (1994) 53–90.
[10] J.H. Lienhard, Snares of pool boiling research: putting our history to use, in: Proc. 10th Int. Heat Transfer Conf., Brighton, UK, vol. 1, 1994, pp. 333–348.
[11] J.H. Lay, V.K. Dhir, Shape of a vapor stem during nucleate boiling of saturated liquids, Trans. ASME J. Heat Transfer 117 (1995) 394–401.
[12] Y.H. Zhao, T. Masuoka, T. Tsuruta, Unified theoretical prediction of fully developed nucleate boiling and critical heat flux based on a dynamic micro layer model, Int. J. Heat Mass Transfer 45 (2002) 3189–3197.
[13] Y. He, M. Shoji, S. Maruyama, Numerical study of high heat flux pool boiling heat transfer, Int. J. Heat Mass Transfer 44 (2001) 2357–2373.
[14] T. Luttich, W. Marquardt, M. Buchholz, H. auracher, Towards a unifying heat transfer correlation for the entire boiling curve, Int. J. Thermal Sci. 43 (2004) 1125–1139.
[15] G. Sateesh, S.K. Das, A.R. Balakrishnan, Analysis of pool boiling heat transfer effect of bubbles sliding on the heating surface, Int. J. Heat Mass Transfer 48 (2005) 1543–1553.
[16] S.K. Das, W. Roetzel, A composite heat transfer model for pool boiling on a horizontal tube at moderate pressure, Can. J. Chem. Eng. 82 (2004) 316–322.
[17] M.G. Cooper, A.J.P. Lloyd, The microlayer in nucleate pool boiling, Int. J. Heat Mass Transfer 12 (1969) 895–913.
[18] C. Ramaswamy, Y. Joshi, W. Nakayama, W.B. Johnson, Semi analytical model for boiling from enhanced structures, Int. J. Heat Mass Transfer 46 (2003) 4257–4269.
[19] S.J.D. Van Stralen, R. Cole, W.M. Sluyter, M.S. Sohal, Bubble growth rates in nucleate boiling of water at sub atmospheric pressures, Int. J. Heat Mass Transfer 18 (1975) 655–669.
[20] J.F. Klausner, R. Mei, D.M. Bernhard, L.Z. Zeng, Vapor bubble departure in forced convection boiling, Int. J. Heat Mass Transfer 36 (1993) 651–662.
[21] A. Sakurai, Mechanism of transition from non boiling to film boiling in various liquids, in: The 31st National Heat Transfer Symposium, Japan, A132, 1994, pp. 31–33.
[22] R.F. Gaertner, Photographic study of nucleate pool boiling on a horizontal surface, Trans. ASME J. Heat Transfer 87 (1975) 17–29.